A fully analytical approach to investigate the electro-viscous effect of the endothelial glycocalyx layer on the microvascular blood flow

Article *in* Clinica chimica acta; international journal of clinical chemistry · July 2017

DOI: 10.1016/j.cca.2017.07.006

CITATION
1

READS
68

4 authors, including:

Hadi Shirazi
Iran University of Science and Technology
21 PUBLICATIONS **140** CITATIONS
SEE PROFILE

Alireza Asnafi
Shiraz University
36 PUBLICATIONS **90** CITATIONS
SEE PROFILE

Clinica Chimica Acta 472 (2017) 5–12

Contents lists available at ScienceDirect

Clinica Chimica Acta

journal homepage: www.elsevier.com/locate/cca

A fully analytical approach to investigate the electro-viscous effect of the endothelial glycocalyx layer on the microvascular blood flow

Arezoo Khosravi[a], Hadi Asgharzadeh Shirazi[b], Alireza Asnafi[c], Alireza Karimi[d,*]

[a] Atherosclerosis Research Center, Baqiyatallah University of Medical Science, Tehran, Iran
[b] School of Mechanical Engineering, Iran University of Science and Technology, Narmak, 16846-13114 Tehran, Iran
[c] School of Mechanical Engineering, Shiraz University, Shiraz 71348-13668, Iran
[d] Department of Mechanical Engineering, Kyushu University, 744 Motooka, Nishi-ku, Fukuoka 819-0395, Japan

ARTICLE INFO

Keywords:
Microvascular
Blood
Electric double layer
Non-Newtonian fluid
Endothelial glycocalyx layer

ABSTRACT

Background: Recently, the glycocalyx lining the endothelial surface has emerged as a structure of fundamental importance to a wide range of phenomena that has undeniable effect on cardiovascular health and disease. With respect to the blood flow in small vessels, it has been experimentally reported that the glycocalyx layer causes additional resistance to the flow.

Methods: The hypothesis of glycocalyx resistance against the blood flow, considered as two-phase layer fluid through a small blood vessel, was theoretically evaluated. To do that, a very thin electric double layer (EDL) was considered and the fluid flow was modeled by the well-known Poisson and Boltzmann equations in micro-fluidics alongside the general Navier-Stokes equation. Finally, a complete analytical solution for this particular case was developed.

Results: The results confirmed the previous findings indicated that the negatively charged glycocalyx layer has no effect on the macro/micro scale blood flow. Here and in the nano-scale, slightly influence was observed and reported in this study.

Conclusion: Moreover, more details about the thin electrically significant layer, close to the EDL, would be delineate to better recognition of electro-viscous effect caused by the endothelial glycocalyx near microvascular walls.

1. Introduction

The blood vessels are the part of the circulatory system that transports blood throughout the human body. There are three major types of blood vessels including arteries, veins and capillaries. Depending on vessel size, different flows as well as wall characteristics have been detected [1]. Blood flow in microvascular networks, generally including arterioles, venules and capillaries, exhibits significantly different characteristics compared to what flows exist in larger vessels in the macrocirculation [2]. The luminal surface of human vessels is lined with a continuous layer of vascular endothelium, which in fact, plays a central role in maintaining vascular integrity. Disorder of endothelial could possibly lead to detrimental vascular disease like atherosclerosis as a chronic inflammatory disease in the artery wall [3].

Numerous pathophysiologic observations have reported that the early stage of atherosclerosis begins by malfunctioning of endothelial cells [4]. Main risk factors of endothelial dysfunctions are high-level of cholesterol intake, cigarette smoking, hypertension, genetic alteration, and bacterial infections [5]. The glycocalyx is another complex subset of luminal surface of human vessels so that continuously decorated on the apical membrane of endothelial cells. In other words, the endothelial cells, especially in small blood vessel, is coated with a gel-like layer of membrane-bound glycoproteins and plasma proteins, named as the glycocalyx layer that adhere to this surface matrix [5]. The thickness of glycocalyx layer could vary from several tens of nanometers to submicron proportional to the radius of the vessel [6–9]. There is also evidence that the glycocalyx, in turn, has a significant influence in various pathologies, like atherosclerosis, vascular disease associated with diabetes, ischemia–reperfusion injury, and sepsis [10]. Previous literature has experimentally stated that the glycocalyx layer may contribute to additional resistance against microvascular flow [11–13]. In experiment researches by Pries et al. [11,12], flow resistance in vivo in small vessels was markedly higher than predicted by in vitro viscosity data. The presence of a thick endothelial surface layer (ESL) has been proposed as the primary cause for this discrepancy. They have also shown that the measured values of flow resistance in microvascular

* Corresponding author.
E-mail addresses: asnafi@shirazu.ac.ir (A. Asnafi), karimi@kyudai.jp (A. Karimi).

http://dx.doi.org/10.1016/j.cca.2017.07.006
Received 4 May 2017; Received in revised form 3 July 2017; Accepted 6 July 2017
Available online 08 July 2017
0009-8981/

Nomenclature

ψ	Electrical field potential	J_0	Zero-order modified Bessel
ρ_e	Net charge density	J_1	First-order modified Bessel
ε	Dielectric constants in the medium	dP/dz	Function of pressure gradient
ε_0	Dielectric constants in the vacuum	u	Axial velocity
n_∞	Bulk ionic concentration	h	Hematocrit fraction
z_i	Valence of type-i ions	μ	Viscosity
K_b	Boltzmann constant	F	Body force
T	Absolute temperature	$\vec{\tau}$	Stress tensor
κ	Debye length	γ	Scalar strain rate
r	Vessel radius	N_A	Avogadro constant
ψ_s	Surface potential	D	Ion's diffusion coefficient
n	non-Newtonian behavioral index	i	Electric current
$\vec{V}$	Flow velocity vector	E_z	Electric field strength

networks are about twice as large as expected from measurements of flow resistance in glass tubes [13]. In their work, flow restriction by the glycocalyx has been stated as a possible reason for this difference. On the other hand, Klitzman et al. [14] have found unexpected low values of hematocrit compared with theoretical prediction from a glass tube model by studying on red cell volume fraction in capillaries of hamster. This discrepancy has been likely explained by assuming a slow-moving plasma layer which was responsible for excluding red blood cell from the layer [14]. Glycocalyx layer is highly negatively charged which constantly interacts with moving plasma phase (treated as an electrolyte) inducing various interfacial and mechanical as well as electrochemical phenomena [15]. This negatively charged of glycocalyx layer is the main reason for that Red blood cells (RBCs), which are also negatively charged, normally do not invade the surrounding areas of the layer because of the electrostatic repulsion.

Despite an important role of endothelial-cell glycocalyx layer (EGL) on the human microcirculation, limited information about it is available, especially in the scope of electro-kinetically. Dey and Sekhar [16] modeled hydrodynamics of flow through EGL with biphasic mixture theory. They demonstrated EGL influences the blood plasma flow rate so that higher depth of EGL would decrease the flow rate through free lumen. Goswami et al. [17] investigated the electro-kinetically modulated peristaltic transport of power-law fluids through a narrow confinement in the form of a deformable tube. There, the fluid is assumed to be divided into two regions as a non-Newtonian core region which is surrounded by a thin wall-adhering layer of Newtonian fluid. Hariprasad et al. [18] is also used a two-dimensional model to simulate the motion and deformation of a single red blood cell (RBC) flowing close

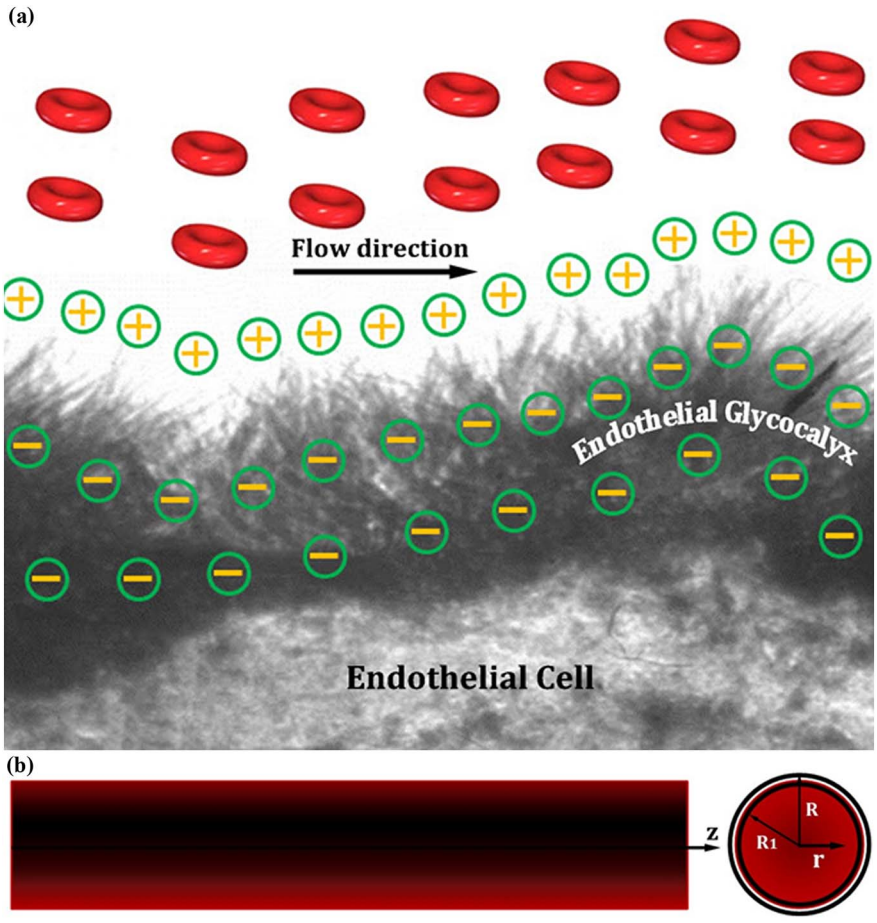

Fig. 1. (a) Schematic illustration of the blood flow throughout a micro vessel in the vicinity of endothelial Glycocalyx layer. (b) Simplified model of a micro vessel and the cylindrical coordinate system (r, θ, z) used in present study.

Table 1
Physical specifications of blood and the parameters chosen in the case study used in this work [15,22,28].

Parameter [unit]	Value	Parameter [unit]	Value
ψ_s [V]	-50×10^{-3}	n_∞ [mol/m^3]	100
ρ [Kg/m^3]	1060	N_A [mol^{-1}]	6.022×10^{23}
μ_c [Pa·(s)^n]	0.0134	z_0	1
μ_p [Pa·s]	1.2×10^{-3}	n	0.785
e [C]	1.6×10^{-19}	dP/dz [Pa/m]	2×10^4
$\varepsilon^*(=\varepsilon \times \varepsilon_0)$ [C/Vm]	5.3×10^{-10}	D [m^2/s]	1.38×10^{-10}
T [K]	300	K_B [J/K]	1.38×10^{-23}

to the wall of a microvessel by considering the effects of a porous endothelial surface layer (ESL) lining the vessel wall. They revealed migration of RBCs away from the wall, caused by the presence of ESL, leads to the formation of a cell-depleted layer near the wall, which has a large effect on the resistance to blood flow in microvessel.

Taking into account what was mentioned and previous works, one can find out glycocalyx layer has undeniable effects on blood flow in small vessels and more investigations about this unique layer are needed for better understanding in terms of blood rheology in response to negatively electrical charges of glycocalyx layer. Hence, the main aim of this paper is to assess the effect of endothelial glycocalyx layer on the micro-vascular blood flow and the electro-viscous effect of this layer. For this purpose, a very thin electric double layer (EDL) was considered and a closed-form solution for the Poisson equation that describes the electrical potential in a dielectric medium was employed. The continuity and the momentum equations in the cylindrical coordinates were considered in order to link both the hydrodynamic and electrochemical fields. After solving equations analytically, the profiles of pressure gradient and electrical potential terms of blood velocity were investigated and discussed for various types of micro-channels.

2. Materials and methods

2.1. Numerical methodology

In this section, the axisymmetric flow in a uniform circular blood vessel exposed to the EDL was considered. It was supposed that the length of the vessel is much bigger than its radius. Fig. 1 shows schematic illustration of a micro blood vessel used in present study. A global cylindrical coordinate system (r, θ, z) is used in which the z-axis is taken to coincide with the central axis of the blood vessel. Moreover, it was assumed that the pressure gradient is independent of the z and r coordinates. This assumption is due to high ratio of length to radius and lack of transverse flow convection.

Table 2
Obtained values for streaming potential, core region velocity induced from electric field and core region velocity in center of the microvessel for different radii values.

R (μm)	R-R_1 (μm)	E_z (mV/m)	u_c (Ψ) (cm/s)	u_c (r = 0)[a] (cm/s)
5	1.5	42.9015	-9.4741×10^{-9}	0.0058
10	1.5	42.9377	-9.4821×10^{-9}	0.0155
50	1.5	42.9667	-9.4885×10^{-9}	0.2679
100	1.5	42.9703	-9.4893×10^{-9}	1.1572
	5.0	42.9703	-9.4893×10^{-9}	1.3578
200	1.5	42.9721	-9.4897×10^{-9}	5.3325
300	1.5	42.9727	-9.4898×10^{-9}	13.2285
400	1.5	42.9730	-9.4899×10^{-9}	25.2956
500	1.5	42.9732	-9.4900×10^{-9}	41.8809

[a] Hint: $u_c(r)=u_c\left(\frac{dp}{dz}\right)(r)+u_c(\psi)$.

2.2. Problem formulation

The Poisson equation describes the electrical potential in a dielectric medium. Generally, it is given by [19]:

$$\nabla^2\psi = -\frac{\rho_e}{\varepsilon\varepsilon_0} \tag{1}$$

where ψ denotes the electrical field potential, ρ_e is the net charge density. The parameters ε and ε_0 are the dielectric constants in the medium and in the vacuum, respectively. Thus, the Poisson equation in the cylindrical coordinates can be rewritten as:

$$\frac{1}{r}\frac{\partial}{\partial r}\left(r\frac{\partial\psi}{\partial r}\right) = -\frac{\rho_e}{\varepsilon\varepsilon_0} \tag{2}$$

By assuming the equilibrium Boltzmann distribution equation is applicable, the number concentration of the type-i ion in a symmetric electrolyte solution is determined via:

$$n_i = n_\infty exp\left(-\frac{z_i e\psi}{k_b T}\right) \tag{3}$$

where n_∞ and z_i are the bulk ionic concentration and the valence of type-i ions, respectively, e is the charge of a proton, K_b is the Boltzmann constant, and T is the absolute temperature. The net volume charge density ρ_e is proportional to the concentration difference between symmetric cations and anions, via [19]:

$$\rho_e = \sum_{i=1}^{2}\rho_i;\rho_i = z_i e n_\infty exp\left(-\frac{z_i e\psi}{k_B T}\right)(i = 1^+,2^-) \tag{4}$$

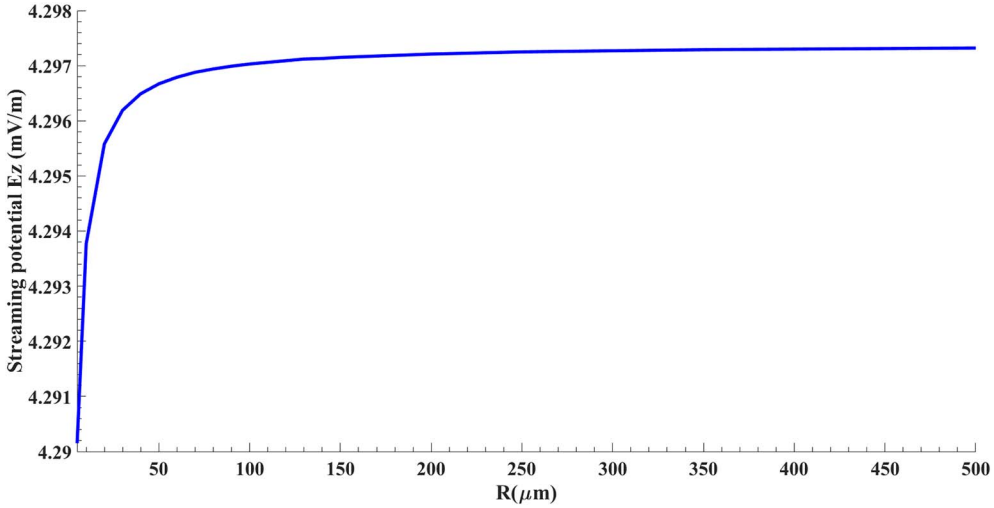

Fig. 2. The profile of streaming potential versus the microvessel radius.

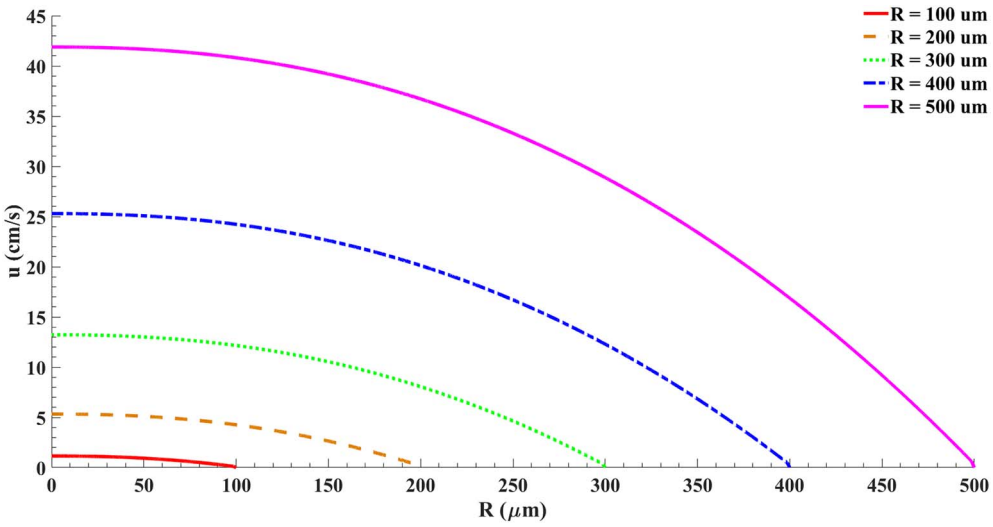

Fig. 3. The velocity profile of blood in microvessel in presence of EDL layer for a range of vessel radius between 5 and 500 μm.

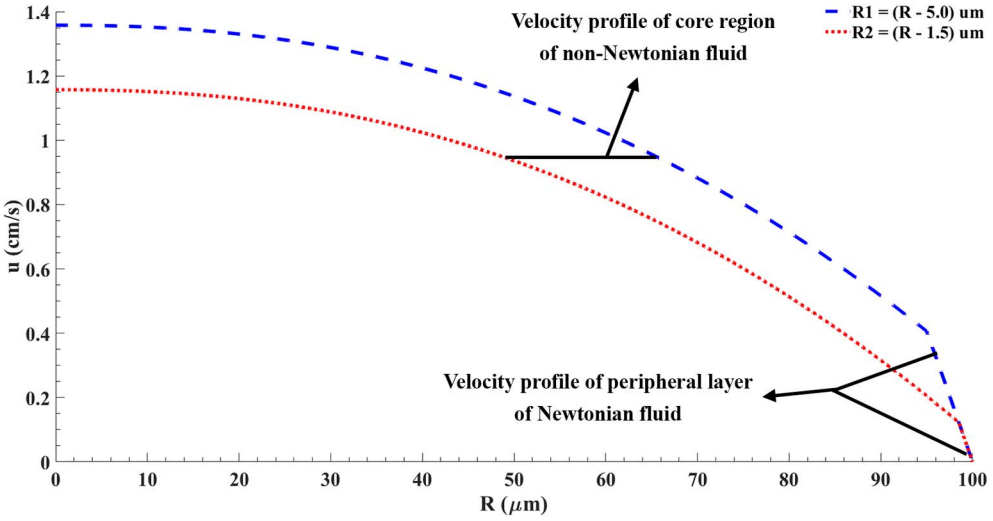

Fig. 4. The effect of parameter R_1 (the distance between microvessel center and two-phase interface) on the velocity profile of the microvessel with $R = 100$ μm.

In the case of having symmetrical ions, i.e. when $z_i = z_1^+ = z_2^- = z_0 =$ constant, and according to the Debye–Hückel approximation for a low surface potential which leads to consider $\frac{z_0 e\psi}{K_B T} \leq 1$, the total charge density reduces to:

$$\rho_e = -\frac{2n_\infty e^2 z_0^2}{k_B T}\psi \tag{5}$$

By substituting Eq. (5) to Eq. (2), the following equation would be achieved:

$$\frac{1}{r}\frac{d}{dr}\left(r\frac{\partial\psi}{\partial r}\right) = \kappa^2\psi;\ \kappa^2 = \left(\frac{2n_\infty e^2 z_0^2}{\varepsilon\varepsilon_0 k_B T}\right)^2 \tag{6}$$

where κ is the reciprocal of the EDL thickness (Debye length). Furthermore, the boundary conditions in terms of $\psi(r)$ are:

$$\frac{d\psi(0)}{dr} = 0;\ \psi(R) = \psi_s \tag{7}$$

in which R and ψ_s indicate the radius and the wall surface potential, respectively. By solving Eq. (6) and considering mentioned boundary conditions in Eq. (7), $\psi(r)$ becomes:

$$\psi(r) = \psi_s \frac{I_0(\kappa r)}{I_0(\kappa R)} \tag{8}$$

where I_0 is the zero-order modified Bessel function of the first kind. After that, the net charge density distribution is given by:

$$\rho_e = -\varepsilon\varepsilon_0\kappa^2\psi_s\frac{I_0(\kappa r)}{I_0(\kappa R)} \tag{9}$$

Now, the continuity and the momentum equations in the cylindrical coordinates were considered in order to link both hydrodynamic and electrochemical fields:

$$\frac{\partial\rho}{\partial t} + \nabla.(\rho\vec{V}) = 0 \quad \text{(Continuity equation)} \tag{10-a}$$

$$\frac{D}{Dt}(\rho\vec{V}) = \nabla.(\vec{\tau}) + \vec{F} \quad \text{(Linear momentum equation)} \tag{10-b}$$

where ρ is the density of the fluid; $\vec{V}$ is the flow velocity vector; $\vec{\tau}$ is the stress tensor and $\vec{F}$ is the body force per unit volume. This force is an electrochemical force and equals to $E_z\rho_e$ in this study. Hence, the axial momentum of the fluid can be satisfied using the assumptions governing the problem such as one-dimensional, steady and incompressible flow as:

$$\frac{1}{r}\frac{\partial(r\tau_{rz})}{\partial r} - \frac{\partial P}{\partial z} + E_z\rho_e = 0 \tag{11}$$

where $\frac{\partial P}{\partial z}$ is the pressure gradient along the cylinder. Since Eq. (11) is a nonlinear ODE differential equation, no explicit response can be obtained in general. Therefore, in order to have an explicit solution, blood in the microvessel is considered as a two-phase fluid consisting of a core region of suspension RBCs (non-Newtonian fluid) and a peripheral layer

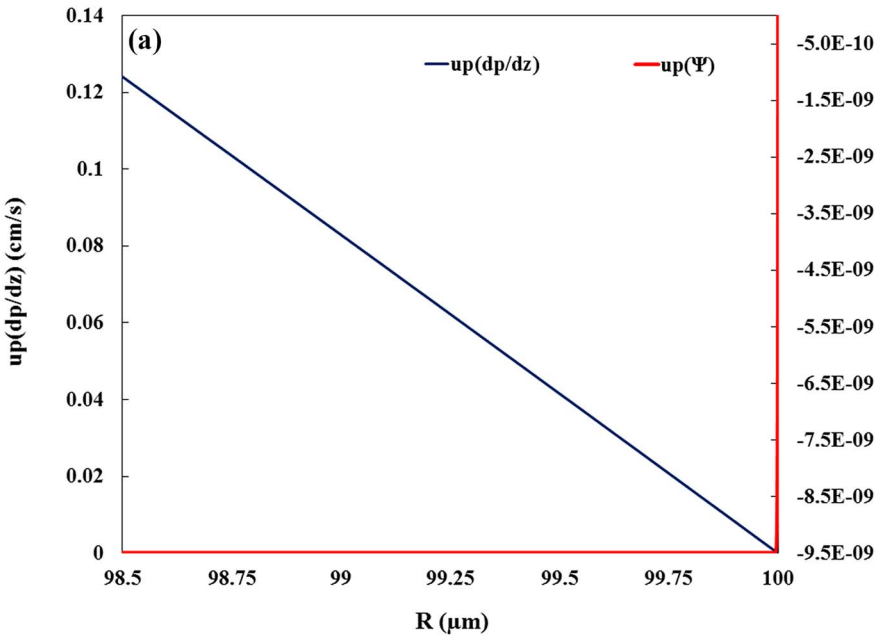

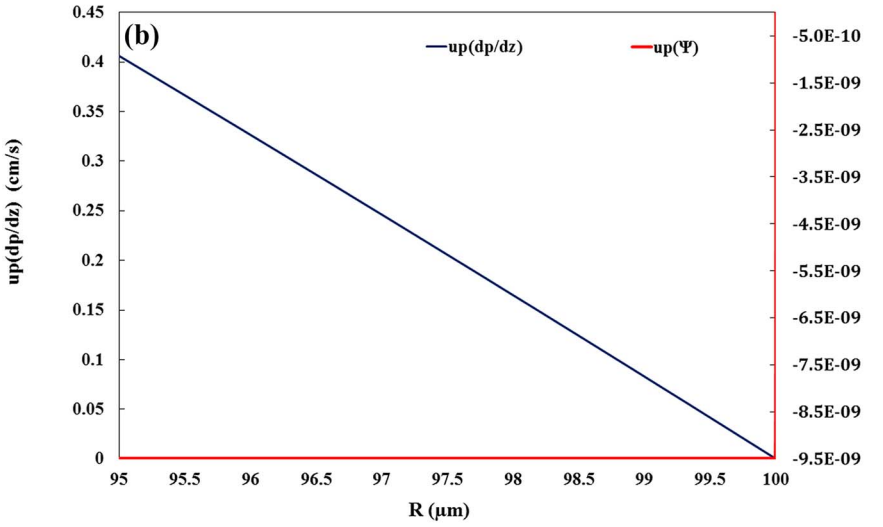

Fig. 5. The profiles of pressure gradient and electrical potential terms of blood velocity in the peripheral layer of Newtonian fluid when a) $R_1 = 1.5\,\mu m$ and b) $R_1 = 5\,\mu m$.

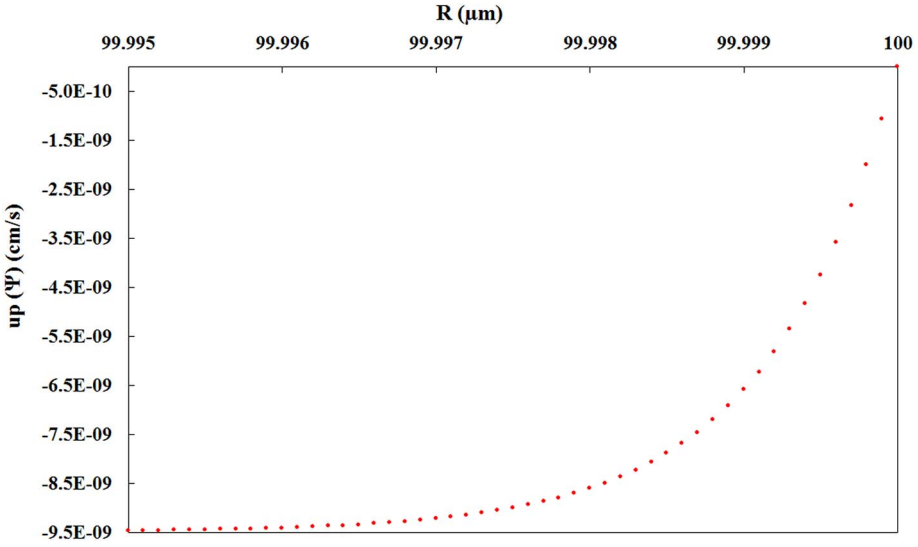

Fig. 6. The profile of blood velocity due to electrical potential in the vicinity of EDL layer.

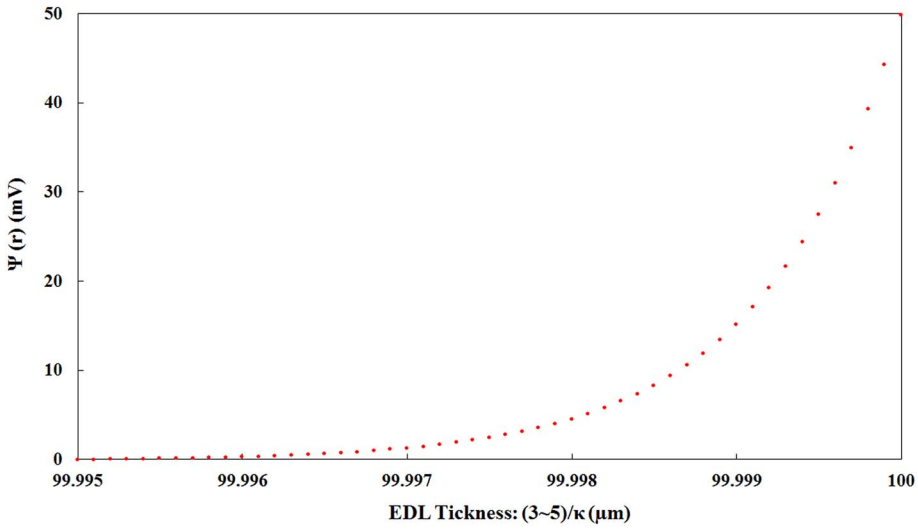

Fig. 7. The profile of electrical potential due to Glycocalyx layer electrical charge along the EDL layer.

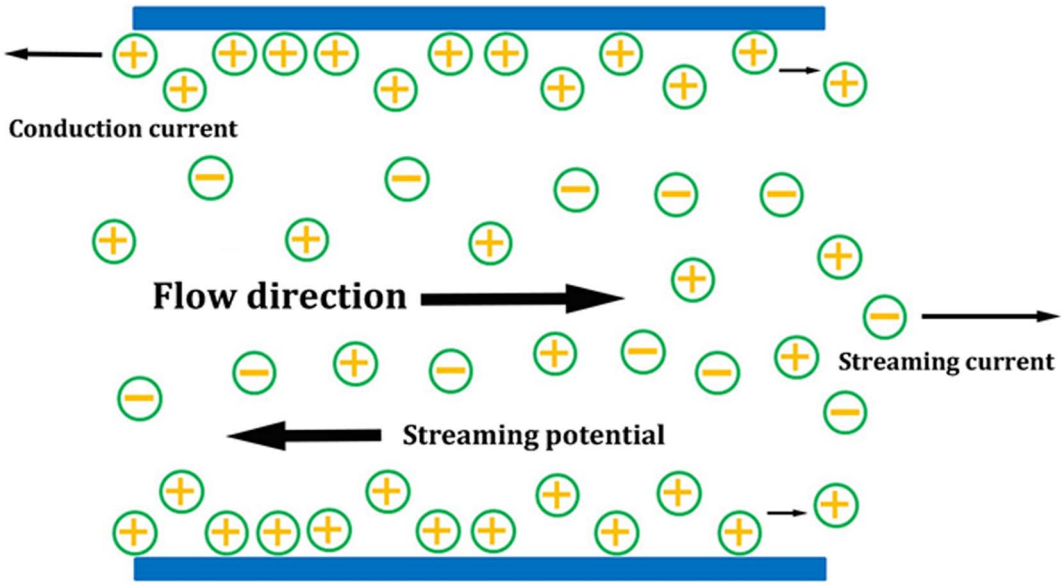

Fig. 8. A schematic diagram of electro-viscose effect in a micro channel.

of plasma (Newtonian fluid). This assumption is based on previous proved recommendations in [20,21]. In other words, blood flow intrinsically exhibits a remarkable two-phase behavior, i.e. a core region of suspension of all the erythrocytes (non-Newtonian fluid) and a peripheral layer of plasma (Newtonian fluid) [20,21]. The formation of a cell-free or cell-depleted layer near the vessel walls stems from repulsion between RBCs and vessel wall (glycocalyx layer). The RBCs show an inclination to migrate away from the vessel walls, leading to the formation of a cell-free layer. Additionally, parabolic profile curvature of flow could be another reason that the RBCs are inclined to migrate in the centerline of vessel. Therefore, blood flow presents a two-phase nature, with a peripheral layer of plasma (Newtonian fluid) and a core region of suspension of erythrocytes (non-Newtonian fluid).

Blood normally indicates non-linear, time-dependent flow characteristics that can be approximately modeled by higher order constitutive relations such as Bingham plastic, a power-law fluid, or a Casson one. Human blood, however, exhibit a very slight Bingham plasticity due to the presence of the protein fibrinogen, but it is mainly considerable in blood samples having relatively higher hematocrit percentages. By considering the normal hematocrit of 40–45%, in general, for all practical purposes the Bingham plastic characteristics of human blood can be neglected, and blood can somewhat accurately be modeled as a power-law fluid which has useful advantages like good representation of fluids with shear-dependent viscosity and simplicity of analysis [22,23]. Therefore, in this paper, the fluid in core region was modeled by a power-law constitutive relationship with the following form:

$$\tau_{rz} = \mu \dot{\gamma}^n \tag{12}$$

where μ is the flow consistency index (may also be appear as μ_c later), and n is the non-Newtonian behavioral index. τ_{rz} and $\dot{\gamma}$ are also the shear stress and the scalar strain rate, respectively. The parameter $\dot{\gamma}$ is also obtained from:

$$\dot{\gamma} = max(\sqrt{D{:}\,D}, \dot{\gamma}_{min});\ D = \frac{1}{2}[\Delta u + u^T] \tag{13}$$

The parameters μ and n appearing in the pertinent constitutive relation are primarily dependent on the hematocrit fraction on certain of the plasma proteins (most notably, the globulins). Under time-independent circumstances, these parameters have such the following form [22]:

$$\mu = C_1 exp(C_2 h) \tag{14-a}$$

$$n = 1\text{-}C_3 h \tag{14-b}$$

where h is the hematocrit fraction in the blood cells. Parameters C_1, C_2, C_3 are dependent on many biological factors such as hematocrit, plasma globulin concentration, plasma protein and blood plasma viscosity [22]. It is also worth noting that the normal ranges of hematocrit in adult male and female are about 42%–54% and 38%–46%, respectively.

Now, by considering the assumption of two-phase fluid consisting of a core region of non-Newtonian fluid (power-law fluid) and a peripheral layer of Newtonian fluid, the both axial velocity profile in response to the two-phase fluid are separately determined by the following equations:

$$\frac{1}{r}\frac{\partial}{\partial r}\left(r\mu_c\left(\frac{\partial u_c}{\partial r}\right)^n\right)-\frac{\partial P}{\partial z}=0 \quad \text{Core region of non}-\text{Newtonian fluid} \tag{15-a}$$

$$\frac{1}{r}\frac{\partial}{\partial r}\left(r\mu_p\left(\frac{\partial u_p}{\partial r}\right)\right)-\frac{\partial P}{\partial z}+E_z\rho_e=0 \quad \text{Peripheral layer of Newtonian fluid} \tag{15-b}$$

The subscripts c and p denote the core region of non-Newtonian fluid and the peripheral layer of Newtonian fluid, respectively.

The boundary conditions for the two-layer model are:

$$\frac{\partial u_c}{\partial r}=0 \quad \text{at}\, r=0 \tag{16-a}$$

$$(\tau_{rz})_c=(\tau_{rz})_p \quad \text{at}\, r=R_1 \tag{16-b}$$

$$u_c=u_p \quad \text{at}\, r=R_1 \tag{16-c}$$

$$u_p=0 \quad \text{at}\, r=R \tag{16-d}$$

where R_1 and R are the radii of core region and peripheral layer, respectively. u_c and u_p are the axial velocities in the central and peripheral regions, i.e. $0 \le r \le R_1$ and $R_1 \le r \le R$, respectively. With the integration of Eqs. (15-a), (15-b) in accordance to the boundary conditions Eqs. (16-a), (16-b), (16-c), (16-d), the velocities in the central core and peripheral layer would be obtained respectively, as:

$$u_c(r)=\frac{r\left(\frac{r}{\mu_c}\frac{dp}{dz}\right)^{\frac{1}{n}}}{2^{\frac{1}{n}}\left(1+\frac{1}{n}\right)}+A \tag{17-a}$$

$$u_p(r)=\frac{r^2}{4\mu_p}\frac{dp}{dz}+\frac{B}{\mu_p}ln(r)+\frac{E_z\varepsilon\varepsilon_0\psi_s(I_0(\kappa r)\text{-}1)}{\mu_p I_0(\kappa R)}+C \tag{17-b}$$

in which parameters A, B and C are:

$$A=\frac{R_1^2}{4\mu}\frac{dp}{dz}-\frac{R_1\left(\frac{R_1}{\mu_c}\frac{dp}{dz}\right)^{\frac{1}{n}}}{2^{\frac{1}{n}}\left(1+\frac{1}{n}\right)}+\frac{E_z\varepsilon\varepsilon_0\psi_s(I_0(\kappa R_1)\text{-}1)}{\mu_p I_0(\kappa R)}+\frac{B}{\mu_p}ln(R_1)+C \tag{18-a}$$

$$B=-\frac{E_z\varepsilon\varepsilon_0\psi_s\kappa^2R_1^2\,\textbf{Hypergeometric 0F1 Regularized}\left[2,\frac{1}{4}\kappa^2R_1^2\right]}{2I_0(\kappa R)} \tag{18-b}$$

$$C=-\left(\frac{R^2}{4\mu}\frac{dp}{dz}+\frac{B}{\mu_p}ln(R)+\frac{E_z\varepsilon\varepsilon_0\psi_s(I_0(\kappa R_1)\text{-}1)}{\mu_p I_0(\kappa R)}\right) \tag{18-c}$$

Due to the complexity of above equations, suitable *hypergeometric* functions were used and embedded in calculations. On the other hand, the electric current caused by electrical potential can also be evaluated using the following equation [24]:

$$i=2\pi\int_0^R\rho_e u r dr+\frac{z_0eD}{k_BT}2\pi\int_0^R(\rho_c\text{-}\rho_p)E_z r dr \tag{19}$$

where D denotes the ion's diffusion coefficient. The first term pertains to bulk convection and the second term is owing to charge migration [25]. Since it is assumed the vessel is long enough, the contribution of the ion concentration gradients in the flow direction could be eliminated. Furthermore, the region far from the wall is at electrically neutral state; so, the term of ρ_c-ρ_p could be simplified to $2z_0en_\infty$ (see also Eq. (4) and the Debye–Hückel approximation). At last, Eq. (19) becomes:

$$i=2\pi\int_{R_1}^R\rho_e u_p r dr+\frac{2\pi R^2z_0^2e^2n_\infty D}{k_BT}E_z \tag{20}$$

By substituting Eqs. (9), (17-a) and (17-b) into Eq. (20), we would have:

$$\begin{aligned}i=&+\frac{\varepsilon\varepsilon_0\pi\psi_s}{2\kappa\mu_p(I_0(\kappa R))^2}\Bigg[2\kappa R^2(I_0(\kappa R))^2\left(\frac{dp}{dz}\text{-}\varepsilon\varepsilon_0E_z\kappa^2\psi_s\right)\\&+2\varepsilon\varepsilon_0E_z\kappa^2\psi_s(\kappa R^2(I_1(\kappa R))^2+2R_1I_1(\kappa R_1))\\&\text{-}4I_0(\kappa R)\left(RI_1(\kappa R)\left(\frac{dp}{dz}\text{-}\varepsilon\varepsilon_0E_z\kappa^2\psi_s\right)+\varepsilon\varepsilon_0E_zR_1\kappa^2I_1(\kappa R_1)\right)\\&\text{-}R_1I_0(\kappa R)\left(\text{-}2\frac{dp}{dz}\kappa R_1I_0(\kappa R_1)+I_1(\kappa R_1)\left(4\frac{dp}{dz}+\frac{dp}{dz}\kappa^2(R_1^2\text{-}R^2)\text{-}4\varepsilon\varepsilon_0E_z\kappa^2\psi_s\right)\right)\\&\text{-}2R_1\varepsilon\varepsilon_0E_z\kappa^2\psi_s(\kappa R_1(I_0(\kappa R_1))^2+2I_0(\kappa R_1)I_1(\kappa R_1))\\&\text{-}2R_1\varepsilon\varepsilon_0E_z\kappa^2\psi_sI_1(\kappa R_1)(\text{-}2+\kappa R_1I_1(\kappa R_1)(2(ln(R)\text{-}ln(R_1))\text{-}1))\Bigg]\\&+\frac{2\pi R^2z_0^2e^2n_\infty D}{k_BT}E_z\end{aligned} \tag{21}$$

Finally, it can be observed that the electrical current includes three terms i.e. the pressure gradient, the surface potential and the ion diffusion. In pressure-driven blood flow, the magnitude of the electric field strength induced by the streaming potential (E_z) is calculated by setting $i=0$ in Eq. (21).

3. Results and discussion

In this section, the application of the derived equations in response to the particular case of relevant physical parameters, as a case study, was perused. These relevant physical parameters are particularly given in Table 1.

Standard anatomy and physiology textbooks reported that the minimum capillary lumen diameter is about 5–7 μm [23] or 4–6 μm [26]. Furthermore, theoretical calculations suggested that the maximum deformation of human red cells, which is normally 7–8 μm in diameter [27], would be about 2.7 μm to pass through capillaries [26]. Therefore, in this paper, the minimum size of microvessel (capillaries) are considered vary between 5 and 500 μm in order to evaluate the effect of endothelial glycocalyx layer on the blood flow throughout such small vessels.

As mentioned earlier, the magnitude of the streaming potential E_z can be calculated from Eq. (21), by setting $i=0$. The values of E_z versus radius of the microvessel are depicted in Fig. 2 and separately listed in Table 2; Now, flow velocity profiles can be plotted as Fig. 3, based on Eqs. (17-a), (17-b) by holding the listed values in Table 1 and amplitudes of E_z (mentioned in Table 2) in response to the multiple sizes of the blood vessel with various range of radius between 5 and 500 μm. With respect to Table 2 and Fig. 3, it is obvious that the total velocity was more influenced by the pressure gradient term of the velocity rather than the term caused by electrical potential. In fact, the latter term has no significant effect on the results. Fig. 4 has explained the effect of R_1 (the distance between microvessel center and two-phase interface) on the velocity profile of the microvessel with $R=100$ μm. This figure has clearly indicated that the parameter R_1 affects noticeably the profile velocity of $u_{c,p}(dp/dz)$ in both core regions of non-Newtonian fluid and peripheral layer of Newtonian fluid; meanwhile Fig. 5 has illustrated that the parameter R_1 has no effect on the velocity of $u_{c,p}(\psi)$.

By dividing the values of results to the micro and nano-scale, (see Fig. 5 and Table 2), one could observe small induced effects of the EDL layer to blood flow in the micro-vessels. Fig. 6 demonstrates that in the nanoscale vicinity of the EDL layer, this effect is quite considerable. In

fact, the thickness of the EDL layer is approximately equal to $\frac{3 \sim 5}{\kappa}$ μm, in which, κ is calculated from Eq. (6). By placing the parameter values from Table 1 into Eq. (6), κ is obtained as 1.185×10^9; therefore, the thickness of the generated EDL layer would be about 2.53 ~ 4.22 nm. As a result, in presence of the EDL layer with nano-scale thickness, the above-mentioned effect is highlighted. Fig. 7 indicates the electrical potential distribution through EDL layer. It should be noted that the EDL thickness is proportional to $\frac{1}{n_\infty}$ where n_∞ denotes the bulk ionic concentration in the equilibrium electro-chemical solution at the neutral state. Therefore, smaller ion concentration in blood which means wider EDL layer, causes a stronger streaming potential; meanwhile, for blood with larger n_∞, it would be vice versa.

The obtained results of this study are in accordance with the findings have been reported in the literature. For example, Liu et al. [15] demonstrated that the negatively charged glycocalyx layer has no effect on the profile velocity of the blood as a non-Newtonian fluid. It is to be noted that there are no more details about generated EDL layers and other terms affected by the EDL layer in previous reports, especially in the nano-scale which the EDL effects are quite clear.

The EDL leads to an apparent viscosity which could be slightly or significantly higher than the true liquid viscosity depending on the amount of streaming potential. This phenomenon is recognized as the electro-viscous effect. To put it more clearly, the presence of the EDL layer applies an electrical force to the ions of the fluid so that the generated force has a substantial influence on the blood flow behavior. In fact, the counter ions in the diffuse part of the EDL layer are transformed thorough the vessel to the downstream ends by hydrostatic pressure of blood circulation.

This movement of ions induces an electrical current in the pressure-driven flow direction which is known as the streaming potential. With respect to this streaming current, there is an electro-kinetic potential, namely streaming potential steering the counter ions in the diffuse layer in opposite direction of the streaming current or pressure-driven directions. This will provide the electrical current as conductive current also. In other words, the liquid molecules will be dragged in opposite direction of pressure-driven flow just by moving the ions of fluid owing to streaming potential. Therefore, in contrast to the pressure-driven flow, the liquid flow is moved. Finally, this countercurrent leads to a decrease flow rate in the pressure drop direction. In this case, a small decrease in the flow rate is seen in comparison to the flow rate predicted by classical fluid mechanics under same conditions. It seems the presence of the EDL layer prepares a higher viscosity in fluid flow with respect to one without this layer. This is generally referred to the electro-viscous effect mentioned earlier in the literature [19]. Fig. 8 briefly depicts the electro-viscous effect in microfluidics field. However, the present work has been illustrated that EDL caused by charged surface of the micro-vessel wall has negligible effect on the blood flow. Hence, one can readily eliminate the terms related to the surface potential, such as $u_{c,p}(\psi)$, in order to lighten the equations structure and spend less computational time.

4. Conclusion

An Analytical solution was provided for studying pressure-driven blood flow in microvascular systems with consideration of the electrochemical effects of the highly electrically charged glycocalyx layer. The results confirm the previous findings indicated that the negatively charged glycocalyx layer has no remarkable effect on the macro/micro scale blood flow. Here, and in the nano-scale, slightly effect was observed and reported in this study. Therefore, the cause of additional resistance which previously reported in some works in the literature [11–13], mainly would be related to other mechanisms of the glycocalyx layer.

Compliance with ethical standards

Funding: None.

Conflict of interest: None.

Ethical approval: This article does not contain any studies with human participants performed by any of the authors.

References

[1] R. Ross, The pathogenesis of atherosclerosis—an update, New England J. Med. 314 (1986) 488–500.
[2] R. Ross, J.A. Glomset, The pathogenesis of atherosclerosis, New England J. Med. 295 (1976) 369–377.
[3] R. Ross, Cell biology of atherosclerosis, Annu. Rev. Physiol. 57 (1995) 791–804.
[4] R. Ross, Atherosclerosis—an inflammatory disease, New England J. Med. 340 (1999) 115–126.
[5] P. Vincent, P. Weinberg, Flow-dependent concentration polarization and the endothelial glycocalyx layer: multi-scale aspects of arterial mass transport and their implications for atherosclerosis, Biomech. Model. Mechanobiol. 13 (2014) 313–326.
[6] R. Chambers, B. Zweifach, Intercellular cement and capillary permeability, Physiol. Rev. 27 (1947) 436–463.
[7] J.H. Luft, Fine Structures of Capillary and Endocapillary Layer as Revealed by Ruthenium Red (Federation proceedings), (1966), pp. 1773–1783.
[8] M.D. Savery, J.X. Jiang, P.W. Park, E.R. Damiano, The endothelial glycocalyx in syndecan-1 deficient mice, Microvasc. Res. 87 (2013) 83–91.
[9] S. Weinbaum, J.M. Tarbell, E.R. Damiano, The structure and function of the endothelial glycocalyx layer, Annu. Rev. Biomed. Eng. 9 (2007) 121–167.
[10] D. Chappell, M. Westphal, M. Jacob, The impact of the glycocalyx on microcirculatory oxygen distribution in critical illness, Curr. Opin. Anaesthesiol. 22 (2009) 155–162.
[11] A. Pries, T.W. Secomb, P. Gaehtgens, J. Gross, Blood flow in microvascular networks. Experiments and simulation, Circ. Res. 67 (1990) 826–834.
[12] A.R. Pries, T.W. Secomb, Microvascular blood viscosity in vivo and the endothelial surface layer, Am. J. Physiol. Heart Circ. Physiol. 289 (2005) (H2657-H64).
[13] A.R. Pries, T.W. Secomb, H. Jacobs, M. Sperandio, K. Osterloh, P. Gaehtgens, Microvascular blood flow resistance: role of endothelial surface layer, Am. J. Physiol. Heart Circ. Physiol. 273 (1997) (H2272-H9).
[14] B. Klitzman, B.R. Duling, Microvascular hematocrit and red cell flow in resting and contracting striated muscle, Am. J. Physiol. Heart Circ. Physiol. 237 (1979) (H481-H90).
[15] M. Liu, J. Yang, Electrokinetic effect of the endothelial glycocalyx layer on two-phase blood flow in small blood vessels, Microvasc. Res. 78 (2009) 14–19.
[16] B. Dey, G. Sekhar, An analytical study on hydrodynamics of an unsteady flow and mass transfer through a channel asymmetrically lined with deformable porous layer, Eur. J. Mech. B. Fluids 55 (2016) 71–87.
[17] P. Goswami, J. Chakraborty, A. Bandopadhyay, S. Chakraborty, Electrokinetically modulated peristaltic transport of power-law fluids, Microvasc. Res. 103 (2016) 41–54.
[18] D. Hariprasad, W. Secomb, Motion of red blood cells near microvessel walls: effects of a porous wall layer, J. Fluid Mech. 705 (2012) 195–212.
[19] D. Li, Electrokinetics in Microfluidics, Academic Press, 2004.
[20] G. Cokelet, Y. Fung, N. Perrone, M. Anliker, Biomechanics: Its Foundation and Objectives, Prentice-Hall, Englewood Cliffs, NJ, 1972.
[21] G. Bugliarello, J. Sevilla, Velocity distribution and other characteristics of steady and pulsatile blood flow in fine glass tubes, Biorheology 7 (1970) 85–107.
[22] S. Das, S. Chakraborty, Analytical solutions for velocity, temperature and concentration distribution in electroosmotic microchannel flows of a non-Newtonian bio-fluid, Anal. Chim. Acta 559 (2006) 15–24.
[23] B.M. Johnston, P.R. Johnston, S. Corney, D. Kilpatrick, Non-Newtonian blood flow in human right coronary arteries: steady state simulations, J. Biomech. 37 (2004) 709–720.
[24] J. Yang, J. Masliyah, D.Y. Kwok, Streaming potential and electroosmotic flow in heterogeneous circular microchannels with nonuniform zeta potentials: requirements of flow rate and current continuities, Langmuir 20 (2004) 3863–3871.
[25] J.H. Masliyah, Electrokinetic Transport Phenomena, Alberta, Oil Sands Technology and Research Authority, 1994.
[26] P. Gaehtgens, Flow of blood through narrow capillaries: rheological mechanisms determining capillary hematocrit and apparent viscosity, Biorheology 17 (1980) 183.
[27] Fung Y-c, Biomechanics: Mechanical Properties of Living Tissues, Springer Science & Business Media, 2013.
[28] F.J. Walburn, D.J. Schneck, A constitutive equation for whole human blood, Biorheology 13 (1976) 201–210.